



## **SEISMIC DAMAGE PREDICTIONS FOR THE GAS DISTRIBUTION SYSTEMS IN GREAT TEHRAN, IRAN**

**Takeshi KOIKE<sup>1</sup>, Shiro TAKADA<sup>2</sup>, Yasuo OGAWA<sup>3</sup>,  
Masaaki MATSUMOTO<sup>4</sup>, Tomoharu TAJIMA<sup>5</sup>, Nemat HASSANI<sup>6</sup>**

### **SUMMARY**

The gas network system in Great Tehran is always threatened by many active faults which historically caused severe earthquakes. Wave effect, liquefaction, fault crossing and landslide are hazard factors that provoke seismic damages of the network system.

The purpose of this study is (a) to estimate the structural damages of the network system in a probabilistic manner, (b) to analyze the system performance of the damaged network and (c) to furnish information on restoration plans of the damaged gas network after the seismic event.

### **INTRODUCTION**

Since seismic ground motion depends on various uncertainties like epicentral location, spatial variations of surface ground thickness, lack of information of SPT data at local sites and so on, probabilistic approaches are taken into consideration to estimate the structural damage of pipeline network segments. These are measured with fragility curves (Shinozuka[1], HAZUS[2] ) which will be developed for their causative factors. The rigorous formulations are developed to obtain the probability of link failure between any two nodes of the network system.

For major earthquakes which are triggered by surrounding major causative faults, the system performance of the damage network are evaluated in terms of major, moderate and minor damage states in order to develop restoration plans and the reinforcement strategy for the damaged network.

The seismic assessment approach of the gas network system is different between the 250 psi/ 100 psi main lines and the 60psi distribution ones. The performance of main lines is assessed with the link damage state which is evaluated with the probability of occurrence of damage state of

---

<sup>1</sup> Professor, Musashi Institute of Technology, Tokyo, JAPAN, E-mail:tkoike@sc.musashi-tech.ac.jp

<sup>2</sup> Professor, Kobe University, Kobe, JAPAN, E-mail:takada@kobe-u.ac.jp

<sup>3</sup> General Manager, Osaka Gas Co., Osaka, JAPAN, E-mail:yasuo-ogawa@osakagas.co.jp

<sup>4</sup> General Manager, Sumitomo Metals Industries, Tokyo, JAPAN,  
E-mail:matsumot-msa@sumitomometals.co.jp

<sup>5</sup> Engineer, Sumitomo Metals Industries, Tokyo, JAPAN, E-mail:tajima-tmh@sumitomometals.co.jp

<sup>6</sup> Professor, PWIT, Tehran, IRAN, E-mail:hassani@pwit.ac.ir

pipe segments furnished as a series system. On the other hand, the performance of low pressure lines, however, is measured with the summation of damage points in each mesh where various diameter pipeline networks are utilized for customer services through the riser pipes connected to each houses.

## SEISMIC HAZARD SURROUNDING TEHRAN CITY AREA

### Major faults causing severe earthquakes

Tehran City is surrounded with major faults which are called as North Tehran, North Ray, South Ray, Mosha and so on as shown in Figure 1. North Tehran and Mosha faults are selected as one of the major faults which might bring significant damages to the lifelines, while North and South Ray faults located inside the city area must be assessed since these faults are located near liquefaction-sensitive zone near the downtown. Other faults (red and green lines) are not included in this analysis because of insignificant dimensions of their fault sizes.

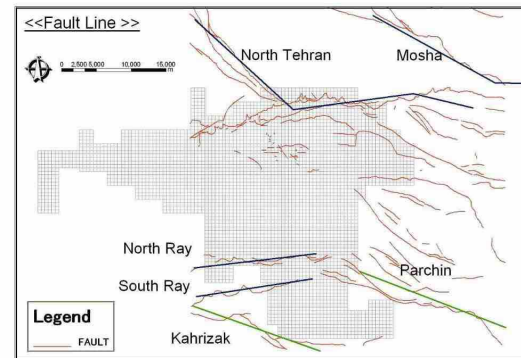


**Figure 1 Major faults surrounding Tehran City**

Once an earthquake occurs from one of these faults, seismic wave motions create large ground strains, while permanent ground deformations may reveal at the hazard areas of fault movement. Liquefaction induced settlement or lateral spreading and landslide may also occur.

Figure 2 shows a simulated result of ground accelerations, if an earthquake occurs at North Tehran, while Figure 3 is a map of liquefaction sensitive areas in Tehran City.

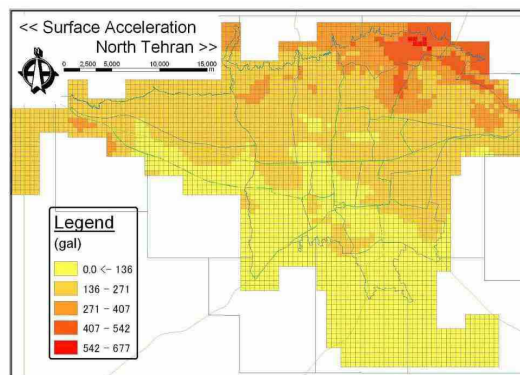


**Figure 2 Ground response map**

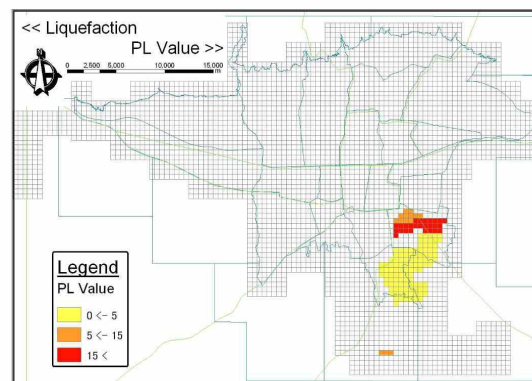


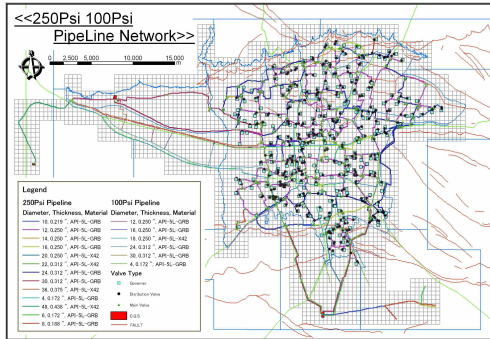
**Figure 3 Liquefaction hazard map**

## PIPELINE NETWORK SYSTEM

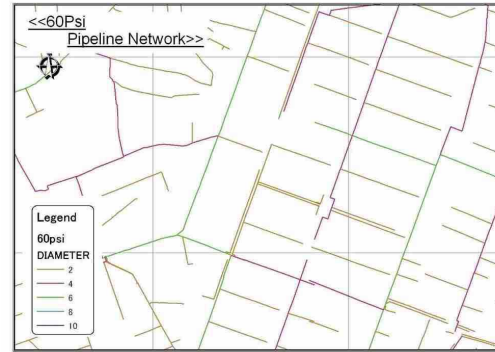
### Modeling of pipeline network

Actual networks of 250 psi and 60 psi gas pipelines shown in Figure 4 and 5 are extended over the whole area of Tehran City. Each 250 psi line has a function of conveying gas flow from one node to the other, while the 60 psi network in one mesh is a gas delivery system from a branch point of the network to customers. These differences in their own function between 250 psi and 60 psi systems appear in making the network models for their analysis. From these point of view,

the 250 psi lines are modeled as a link connecting two neighboring nodes, while the 60 psi lines in one mesh are defined as a structural but scattered assembly of various pipelines with riser pipes, curb valves and control valve stations.



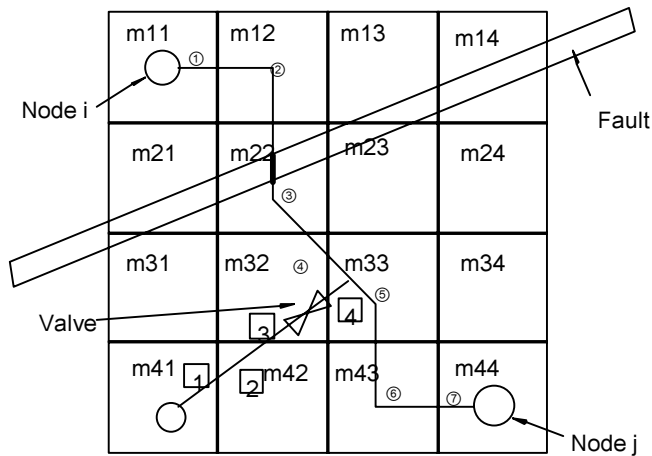
**Figure 4 Distribution main system**



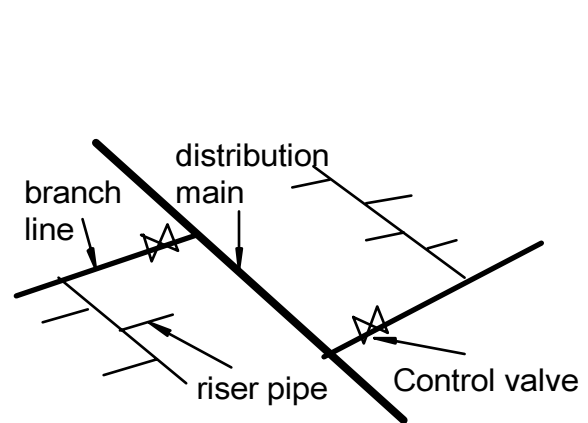
**Figure 5 network for customer services**

Figure 6 is furnished for the 250 psi distribution main lines, while Figure 7 is for the 60 psi distribution system in one mesh. In this study, the mesh (m22) in Figure 6 is selected as a schematic example, for the 60 psi system of Figure 7.

In the following analysis, the 250 psi line between node i and j in Figure 6 is divided into 7 portions which belong to their corresponding 7 meshes. The line in each mesh is also divided into many segments of a straight pipe (Wp), a bend(B), a fault crossing zone (F), a liquefaction induced settlement zone (Lp for pipe and LB for bend), landslide (LS) and valve station (H), respectively. The 60 psi network is modeled for a single mesh which has various diameters of pipeline networks including branch lines, riser pipes (R ), curb valves (CB) and their crossing points to fault lines or liquefaction area.



**Figure 6 Modeling of main lines**



**Figure 7 Modeling of network to customer services**

### Damage estimations

Three different modes are introduced to describe the damage states of one link as major, moderate and minor damage states (Shinozuka [3]) which are defined as follows;(1) major damage is defined as the state when at least one pipe segment is in major damage state along the pipeline; (2) moderate damage is defined as the state when all the pipe segments are not in the major damage state and also not in the minor

damage state; and (3) minor damage is defined as the state all the pipe segments along the pipeline are in the minor damage state.

The definitions of these damage modes are formulated as follows:

#### Definition of damages

$$\begin{aligned}
 p_f(\text{major damage}|EQ_n) &= P(\text{major damage along the single link of } L_{ij}|EQ_n) \\
 &= 1 - P(\text{no major damage in every link segment along the single link of } L_{ij}|EQ_n) \\
 &= 1 - \prod_{k=1}^{k=NL_{ij}} \{1 - P[d_k = \text{major damage}|EQ_n]\}
 \end{aligned} \tag{1}$$

$$\begin{aligned}
 p_f(\text{minor damage}|EQ_n) &= P(\text{minor damage in every link segment along the single link of } L_{ij}|EQ_n) \\
 &= \prod_{k=1}^{k=NL_{ij}} P[d_k = \text{minor}|EQ_n]
 \end{aligned} \tag{2}$$

$$p_f(\text{moderate damage}|EQ_n) = 1 - p_f(\text{major damage}|EQ_n) - p_f(\text{minor damage}|EQ_n) \tag{3}$$

where

$d_k$  indicates the damage state of the  $k$ -th link segment,  $L_{ij}(k)$  indicates the  $k$ -th link segment along the  $L_{ij}$ ,  $NL_{ij}$  is the total number of pipe segments in the single link  $L_{ij}$ .

#### Probability of occurrence of damage states for the link segments of 250 psi main lines

##### 1) Pipe

$$\begin{aligned}
 p_f^{wp}(\text{major damage of the } k\text{-th link segment } L_{ij}(k)|EQ_n) &= \bigcup_{x \in m22} P[\varepsilon_p > \varepsilon_{cr}^{major} | E\{\varepsilon_G(x)\}] P[E\{\varepsilon_G(x)\}|EQ_n] \\
 &= 1 - \exp\left\{-\int_0^{l_{ij}^k} \nu_s P[\varepsilon_p > \varepsilon_{cr}^{major} | E\{\varepsilon_G(x)\}] P[E\{\varepsilon_G(x)\}|EQ_n] dx\right\}
 \end{aligned} \tag{4.a}$$

$$\begin{aligned}
 p_f^{wp}(\text{minor damage of the } k\text{-th link segment } L_{ij}(k)|EQ_n) &= \bigcap_{x \in m22} P[\varepsilon_p < \varepsilon_{cr}^{minor} | E\{\varepsilon_G(x)\}] P[E\{\varepsilon_G(x)\}|EQ_n] \\
 &= \exp\left\{-\int_0^{l_{ij}^k} \nu_s \{1 - P[\varepsilon_p < \varepsilon_{cr}^{minor} | E\{\varepsilon_G(x)\}] P[E\{\varepsilon_G(x)\}|EQ_n]\} dx\right\}
 \end{aligned} \tag{4.b}$$

where

$E\{\varepsilon_G(x)\}$  means the event of uncertain free field strain  $\varepsilon_G(x)$ ,  $\nu_s$  is a rate of occurrence per  $km$  and  $l_{ij}^k$  is an interval of the  $k$ -th mode between the nodes  $i$  and  $j$ .

##### 2) Fault crossing

$$\begin{aligned}
 p_f^F(\text{major damage of the } k\text{-th link segment } L_{ij}(k)|EQ_n) &= \bigcup_{x \in m22} P[\varepsilon_F > \varepsilon_{cr}^{major} | E\{\Delta_F(x)\}] P[E\{\Delta_F(x)\}|EQ_n] \\
 &= 1 - \prod_{m=1}^{n_F} \{1 - P[\varepsilon_F > \varepsilon_{cr}^{major} | E\{\Delta_F(x_m)\}] P[E\{\Delta_F(x_m)\}|EQ_n]\}
 \end{aligned} \tag{5.a}$$

$$\begin{aligned}
p_f^F(\text{minor damage of the } k\text{-th link segment } L_{ij}(k)|EQ_n) &= \bigcap_{x \in m22} P[\varepsilon_F < \varepsilon_{cr}^{\text{minor}} | E\{\Delta_F(x)\}] P[E\{\Delta_F(x)\} | EQ_n] \\
&= \prod_{m=1}^{n_F} P[\varepsilon_F < \varepsilon_{cr}^{\text{minor}} | E\{\Delta_F(x_m)\}] P[E\{\Delta_F(x_m)\} | EQ_n]
\end{aligned} \tag{5.b}$$

where

$E\{\Delta_F(x)\}$  means the event of uncertain fault dislocation and  $n_F$  is the number of the fault crossing points in the  $m22$ -th mesh (to be an example mesh).

#### Probability of occurrence of damage states for the $k$ -th link

Once the probability of damage states for each mesh along the  $k$ -th link are furnished in Eqs.(4) and (5), the probability of damage states of the  $k$ -th link can be formulated as the series system of those in each mesh as follows:

$$\begin{aligned}
P[d_k = \text{major} | EQ_n] &= 1 - \{1 - p_f^{wp}(\text{major damage of the } k\text{-th segment } L_{ij} | EQ_n)\} \\
&\cdot \{1 - p_f^{WB}(\text{major damage of the } k\text{-th segment } L_{ij} | EQ_n)\} \cdot \{1 - p_f^F(\text{major damage of the } k\text{-th segment } L_{ij} | EQ_n)\} \\
&\cdot \{1 - p_f^{Lp}(\text{major damage of the } k\text{-th segment } L_{ij} | EQ_n)\} \cdot \{1 - p_f^{LB}(\text{major damage of the } k\text{-th segment } L_{ij} | EQ_n)\} \\
&\cdot \{1 - p_f^{LS}(\text{major damage of the } k\text{-th segment } L_{ij} | EQ_n)\} \cdot \{1 - p_f^H(\text{major damage of the } k\text{-th segment } L_{ij} | EQ_n)\}
\end{aligned} \tag{6}$$

$$\begin{aligned}
P[d_k = \text{minor} | EQ_n] &= p_f^{wp}(\text{minor damage of the } k\text{-th segment } L_{ij} | EQ_n) \\
&\cdot p_f^{WB}(\text{minor damage of the } k\text{-th segment } L_{ij} | EQ_n) \\
&\cdot p_f^F(\text{minor damage of the } k\text{-th segment } L_{ij} | EQ_n) \\
&\cdot p_f^{Lp}(\text{minor damage of the } k\text{-th segment } L_{ij} | EQ_n) \\
&\cdot p_f^{LB}(\text{minor damage of the } k\text{-th segment } L_{ij} | EQ_n) \\
&\cdot p_f^{LS}(\text{minor damage of the } k\text{-th segment } L_{ij} | EQ_n) \\
&\cdot p_f^H(\text{minor damage of the } k\text{-th segment } L_{ij} | EQ_n)
\end{aligned} \tag{7}$$

#### Probability of occurrence of damage states for the 60 psi network system

The probability of occurrence of damage states for the 60 psi network must be given for each diameter denoted by  $D$ , so that the probability for each diameter pipeline in the  $k$ -th mesh can be formulated as follows:

##### Pipe

$$\begin{aligned}
&p_f^{wp}(\text{major damage of a pipe with its diameter } D \text{ in the } k\text{-th mesh } m_k | EQ_n) \\
&= \bigcup_{x \in m22} P[\varepsilon_p(D) > \varepsilon_{cr}^{\text{major}} | E\{\varepsilon_G(x)\}] P[E\{\varepsilon_G(x)\} | EQ_n] \\
&= 1 - \exp\{-l(m_k) \nu_S(D) P[\varepsilon_p(D) > \varepsilon_{cr}^{\text{major}} | E\{\varepsilon_G(m_k)\}] P[E\{\varepsilon_G(m_k)\} | EQ_n]\}
\end{aligned} \tag{8.a}$$

$$\begin{aligned}
&p_f^{wp}(\text{minor damage of a pipe with its diameter of } D \text{ in the } k\text{-th mesh } m_k | EQ_n) \\
&= \bigcap_{x \in m22} P[\varepsilon_p(D) < \varepsilon_{cr}^{\text{minor}} | E\{\varepsilon_G(m_k)\}] P[E\{\varepsilon_G(m_k)\} | EQ_n] \\
&= \exp\{-l(m_k) \cdot \nu_S \{1 - P[\varepsilon_p < \varepsilon_{cr}^{\text{minor}} | E\{\varepsilon_G(x)\}] P[E\{\varepsilon_G(x)\} | EQ_n]\}
\end{aligned} \tag{8.b}$$

where  $\nu_s(D)$  is a rate of occurrence per km for a pipeline with diameter of  $D$ ,  $l(m_k)$  is a length of pipeline and,  $\varepsilon_G(m_k)$  is the maximum ground strain in the  $k$ -th mesh, respectively

*Riser pipe*

$$\begin{aligned} & p_f^R(\text{major damage of a riser pipe in the } k\text{-th mesh } m_k | EQ_n) \\ &= \bigcup_{x \in m_{22}} P[\alpha_G(m_k) > \alpha_{cr}^{major} | E\{\alpha_G(m_k)\}] P[E\{\alpha_G(m_k)\} | EQ_n] \\ &= 1 - \left\{ 1 - P[\alpha_G(m_k) > \alpha_{cr}^{major} | E\{\alpha_G(m_k)\}] P[E\{\alpha_G(m_k)\} | EQ_n] \right\}^{n_R} \end{aligned} \quad (9.a)$$

$$\begin{aligned} & p_f^R(\text{minor damage of a riser pipe in the } k\text{-th mesh } m_k | EQ_n) \\ &= \bigcap_{x \in m_{22}} P[\alpha_G(m_k) < \alpha_{cr}^{minor} | E\{\alpha_G(m_k)\}] P[E\{\alpha_G(m_k)\} | EQ_n] \\ &= \left\{ P[\alpha_G(m_k) < \alpha_{cr}^{minor} | E\{\alpha_G(m_k)\}] P[E\{\alpha_G(m_k)\} | EQ_n] \right\}^{n_R} \end{aligned} \quad (9.b)$$

where  $\alpha_G(m_k)$  is a ground acceleration in the  $k$ -th mesh, and  $n_R$  is a number of riser pipes.

## FRAGILITY CURVES

The probability of damage states for 250 psi and 60 psi pipelines are formulated in Eqs.(1) to (9), in which the integrand of each equation must be assessed with the probability of occurrence of damage state for external load conditions such as ground acceleration, ground strain, fault dislocation, settlement displacement and so on. The concept of fragility curve can be developed for these conventional calculations.

As an example, the fragility curve of a pipeline is calculated in the following way.

Since the probability of failure is given by the probability of event  $Q > R$  with the external load condition  $E\{Y\}$ , we obtain the following formula with the safety index  $\beta_Z$  through  $Z = R - Q(Y)$ :

$$P[Q > R | E\{Y\}] = P[R - Q(Y) < 0] = P[Z < 0] = \Phi[-\beta_Z] \quad (10)$$

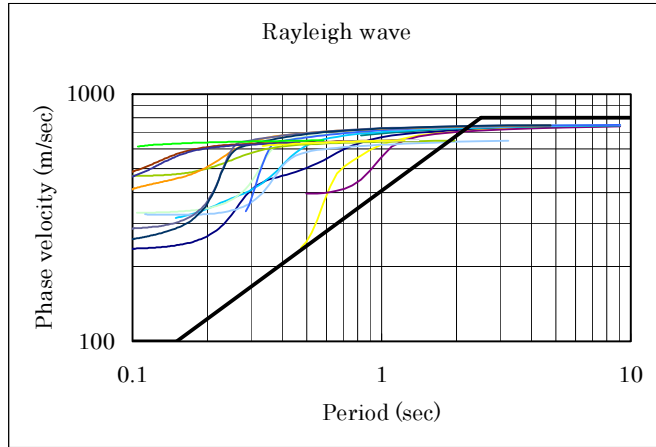
in which, in the case of wave effect, the following values are adopted in the calculation:

$$\begin{aligned} Q &= \varepsilon_p = \alpha \varepsilon_G(Y) \quad , \quad R = \varepsilon_{cr}^{major} = 3\% \quad \text{where} \quad \varepsilon_G(Y) = \frac{\max|\dot{u}(t)|}{C} \\ \mu_{\varepsilon_G} &= \frac{E[\dot{u}_{\max}]}{\mu_C} \quad , \quad \sigma_{\varepsilon_G} = \mu_{\varepsilon_G} \cdot \delta_{\varepsilon_G} \end{aligned} \quad (11)$$

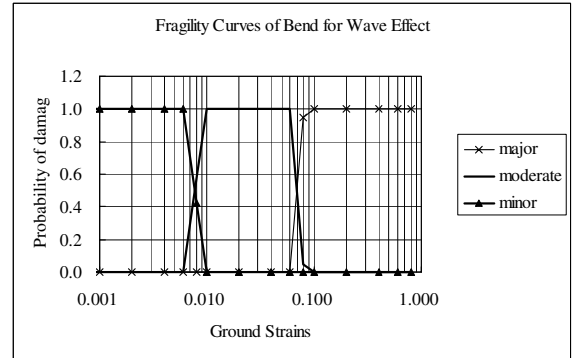
where  $Q$  is pipe strain,  $R$  is the critical strain for major damage of pipeline,  $\varepsilon_G(Y)$  is the ground strain to be given as the ratio of the particle velocity to the phase velocity  $C$  of the surface ground, and  $\alpha$  is a conversion factor (Koike [4]) to estimate the pipe strain from the ground strain,  $C$  is a phase velocity of Rayleigh wave in the surface ground of Tehran city, and  $\mu_X$ ,  $\sigma_X$ ,  $\delta_X$  are mean, standard deviation and coefficient of variation of random variable  $X$ .

Figure 8 is the phase velocity (the first mode) of Rayleigh wave for the surface ground of Tehran City in which 20 soil layer models are selected as a typical surface layer of Tehran City. The bulk line of this figure is the phase velocity curve used in the guideline of the seismic design of gas pipelines (JGA [5]). This bulk line appears to be the lowest curve of the phase velocities in

Tehran City. In the numerical calculation of this study, this bulk line is adopted as the basic phase velocity of Tehran City.



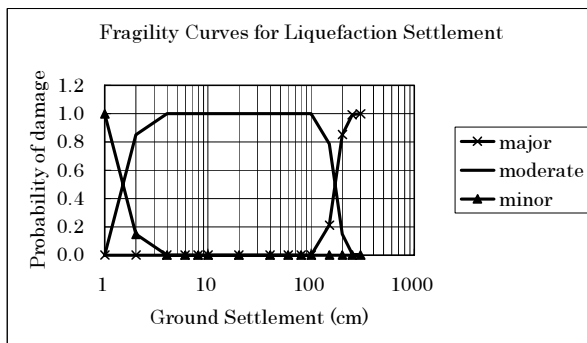
**Figure 8 Phase velocities of surface ground in Tehran City**



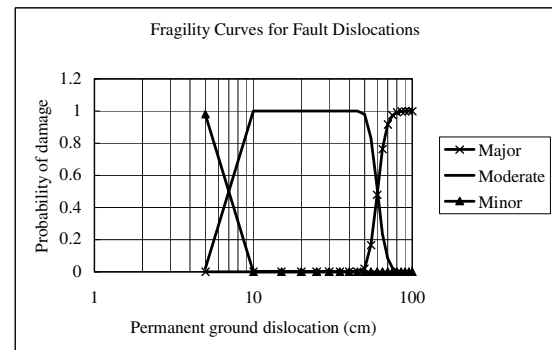
**Figure 9 Fragility curves of bends for wave effect**

Figure 9 is a schematic example of fragility curves of bends for wave effect. Bends are always found in a pipeline and their bending strains are intensified at bending corners. Fragility curve suggests that major damage may initiate when the ground strain exceeds several percentage of strain level.

Figures 10 and 11 are fragility curves for liquefaction induced settlement and fault dislocation, respectively. These figures are given for the permanent ground deformation in one mesh.



**Figure 10 Fragility curves for liquefaction settlement**



**Figure 11 Fragility curves for fault dislocation**

## NUMERICAL RESULTS

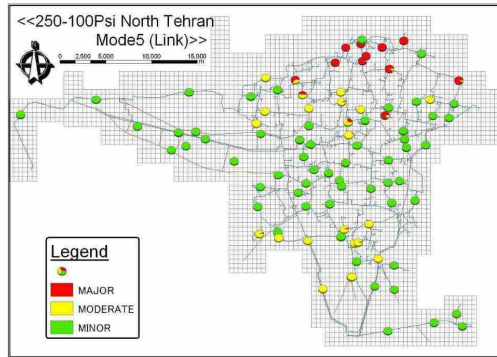
The gas pipeline network system of Tehran City is utilized for the numerical study. The pipelines uses arc-welded steel pipes of API 5LX, with diameters of 50 mm to 1200 mm. Poly-ethylene pipes were also used in some portion of the service lines.

The performance of riser pipes for seismic forces given from housing attached herewith were examined with a full-scale riser pipe model.

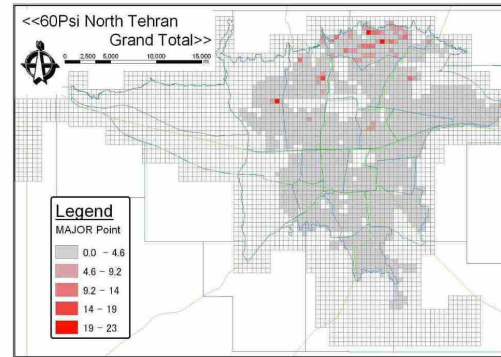


Figure 12 shows the damage states of distribution main lines when a simulated earthquake occurs along North Tehran fault line. This figure suggests that North Tehran fault may threaten major damage to the northern part of Tehran City more than the southern part. Figure 13 also shows that the major damage for 60 psi network is concentrated at the northern part.

Simulation studies were conducted for severe earthquakes triggered from major 4 faults and others in order to identify the most damaged area.



**Figure 12 Damage distributions of main lines**



**Figure 13 Damage point distribution in 60psi networks**

## CONCLUSIONS

This study developed a seismic assessment method of an actual gas pipeline network in which various damage modes of wave effect, fault crossing, liquefaction hazard and landslide are taken into consideration. Discussion was conducted for the appropriate modeling of the pipeline networks in high pressure and low pressure lines, respectively.

One may suggest that the fragility curve approach is effective to estimate the structural damages of the network system in a probabilistic manner, and that, for the restoration planning just after earthquake, the damage states of the link connectivity as the main line is effective, but the information of total amount of damage points in each mesh is more effective in distribution networks for customers services. This result suggests that the appropriate definition of system performance of the pipeline network is different by its own function of the network system.

## ACKNOWLEDGEMENT

This study was conducted by the Investigation Research Committee for Earthquake Resistance Evaluation of Tehran Gas Supply System headed by Professor Shiro Takada of Kobe University, as part of the "Research Project for Strengthening and Control of Tehran Gas Network Against Earthquake" (fiscal 2002 through 2003), commissioned by National Iranian Gas Company(NIGC) and Greater Tehran Gas Company(GTGC). We would like to express our gratitude to all related parties, including authorities, experts and staff of NIGC and GTGC for their kind assistance in our study.



## REFERENCES

1. Shinozuka, M., Feng M. Q., Lee J. and Nakamura T. "Statistical analysis of fragility curves." ASCE, EM, Vol.126, No.12, 2000.
2. Federal Emergency Management Agency "HAZUS 99 Earthquake Loss Estimation Methodology." 1999.
3. Shinozuka, M. and Koike T. "Seismic risk analysis on system connectivity of underground lifelines." JSCE, No.311, 1981.
4. Koike, T. and Imai T. "Structural displacement analysis of buried pipelines against strong earthquake ground motions." Journal of Structural Engineering, JSCE, Vol.44A, 1998.
5. Japan Gas Association "The guideline of seismic design for high pressure gas pipelines." JGA, 2000.